Journal of Alloys and Compounds 518 (2012) 58–62

Contents lists available at SciVerse ScienceDirect

Journal of Alloys and Compounds

journal homepage: www.elsevier.com/locate/jallcom

Synthesis of flower-like $LiMnPO_4$/C with precipitated $NH_4MnPO_4 \cdot H_2O$ as precursor

Jiali Liu, Dongge Hu, Tao Huang, Aishui Yu*

Department of Chemistry and Shanghai Key Laboratory of Molecular Catalysis and Innovative Materials, Institute of New Energy, Fudan University, 2205 Songhu Road, Shanghai 200433, China

ARTICLE INFO

Article history:
Received 5 November 2011
Received in revised form
21 December 2011
Accepted 23 December 2011
Available online 31 December 2011

Keywords:
$NH_4MnPO_4 \cdot H_2O$
Flower-like morphology
$LiMnPO_4$/C
Lithium ion battery
Discharge capacity

ABSTRACT

Ammonium magnesium phosphate monohydrate ($NH_4MnPO_4 \cdot H_2O$) precursor was prepared by a novel precipitating process with manganese citrate complexes as intermediate. The morphology of the precursor observed by Scanning Electron Microscope (SEM) was flower-like which was self-assembled by plate-like particles. Further analysis by X-ray diffraction (XRD) revealed that the lattice of the plate crystal was orientated along (0 1 0) plane. By solid-state reaction of the precursor, with lithium acetate and glucose as carbon source, pure olivine structured $LiMnPO_4$/C composite was obtained and meanwhile, the original flower-like morphology could be retained.

1. Introduction

As a promising cathode material for lithium ion batteries, olivine structured lithium transition metal phosphate $LiMPO_4$ (M = Fe, Co, Mn) has attracted lots of attentions [1–5]. It has three-dimensional framework which stabilizes the structure during the lithium insertion and desertion [6]. Hence, this family of compounds delivers better reversible capacities and higher stability than any other ones [7,8]. In addition, its considerable advantages like low cost and environmental friendly make it have great potential to be applicated in large-scale, such as EV and HEV [9–12].

Lithium manganese phosphate ($LiMnPO_4$) has a flat 4.1 V plateau versus Li^+/Li which is regarded as a good alternative for $LiCoO_2$ [1,13–16]. And higher redox voltage for Mn^{2+}/Mn^{3+} also indicates its higher energy density than $LiFePO_4$ [17]. Up to now, tremendous studies have been conducted on $LiFePO_4$, focusing on the synthetic routes to improve the electrochemical performance or control the morphology [18–23]. Nevertheless, there have been few previous studies on the novel morphology for $LiMnPO_4$ compared to $LiFePO_4$. Fang et al. prepared rod and plate like $LiMnPO_4$ which range from 1 μm to 100 nm by hydrothermal method, and it was found that the morphology related to the reaction condition during hydrothermal process [24]. Choi et al. synthesized nanoplate $LiMnPO_4$ controlled by molten hydrocarbon assisted solid-state reaction [16]. Tarascon produced various types of $LiMnPO_4$ using ionic liquid as reacting media which should be conducted at temperature range of 220–250 °C [25].

$NH_4MPO_4 \cdot H_2O$ precursor based method for preparing $LiMPO_4$ (M = Fe, Mn, Co) has been reported in previous literatures. Tirado synthesized NH_4CoPO_4 by precipitating method, and then $LiCoPO_4$ was obtained through solid-state procedure [26,27]. Bramnik precipitated plate-like $NH_4MnPO_4 \cdot H_2O$ from aqueous solution and revealed that the pH value for the precipitating process would not influence the basic morphology of $NH_4MnPO_4 \cdot H_2O$ [28]. Here, we suggested a novel method to synthesize flower-like $NH_4MnPO_4 \cdot H_2O$ and $LiMnPO_4$, and that the electrochemical behavior were also reported.

2. Experimental

2.1. Synthesis of materials

0.002 mol manganese acetate tetrahydrate ($Mn(CH_3COO)_2 \cdot 4H_2O$, Sinopharm Chemical Reagent Co. Ltd., Shanghai, AR) and 0.002 mol citric acid monohydrate (Sinopharm Chemical Reagent Co. Ltd., Shanghai, AR) were dissolved in 10 ml deionized water, respectively. Then under magnetic stirring, the latter solution was poured into the former one, white precipitation appeared immediately in the mixed solution. After stirring for 6 h, 10 ml deionized water containing 0.002 mol ammonium dihydrogen phosphate ($NH_4H_2PO_4$, Sinopharm Chemical Reagent Co. Ltd., Shanghai, AR) was added into it and was stirred intensely for another 30 min. The pH value of the resulting solution was then adjusted to the range of 10.2–10.7 by adding ammonia ($NH_3 \cdot H_2O$, Zhitang Chemmicals Co. Ltd., Taicang) to precipitate $NH_4MnPO_4 \cdot H_2O$. After stirring for a short while, the obtained precipitate was

* Corresponding author. Tel.: +86 21 51630320; fax: +86 21 51630320.
E-mail address: asyu@fudan.edu.cn (A. Yu).

0925-8388/$ – see front matter © 2012 Elsevier B.V. All rights reserved.
doi:10.1016/j.jallcom.2011.12.134

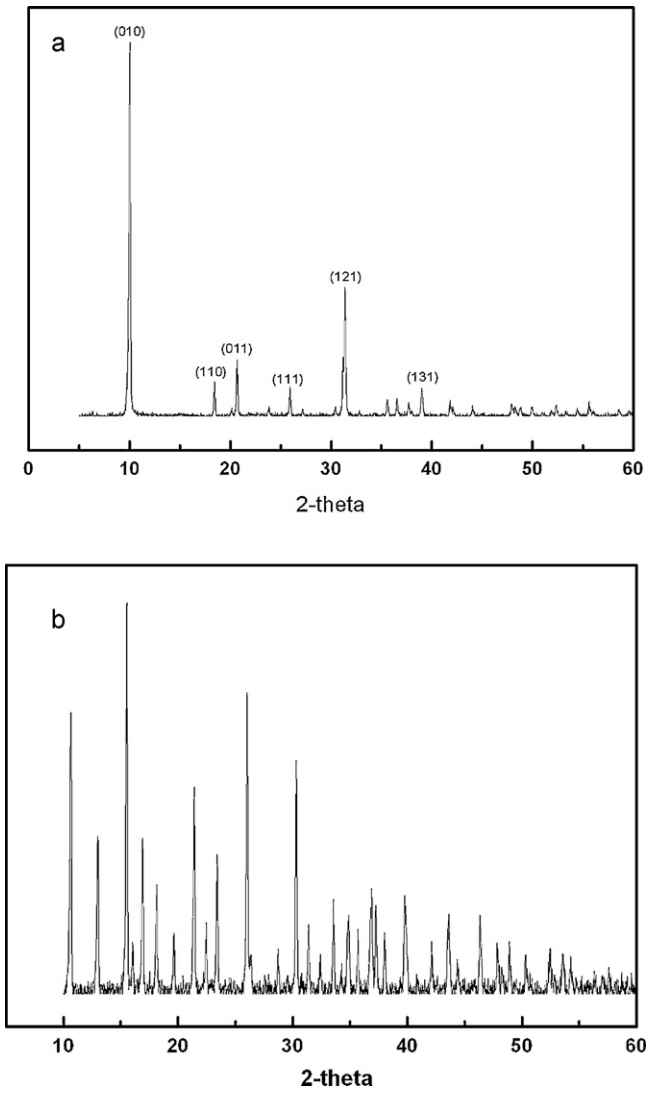

Fig. 1. (a) The XRD data of as-prepared $NH_4MnPO_4{\cdot}H_2O$. (b) The obtained white precipitate obtained by adding citric acid.

filtered and washed for several times with distilled water and acetone, and dried at 80 °C overnight.

With respect to the as-prepared $NH_4MnPO_4{\cdot}H_2O$, the stoichiometric amounts of lithium acetate dehydrate ($LiAC{\cdot}2H_2O$, Sinopharm Chemical Reagent Co. Ltd., Shanghai, AR) and glucose (Sinopharm Chemical Reagent Co. Ltd., Shanghai) (1:9 weight ratio to that of $LiMnPO_4$ to be yielded) were mixed. After milling for 1 h, the precursors were heated at 310 °C for 1 h in the atmosphere of Ar containing 5% H_2. After being cooled down to room temperature, the products were milled again for another 30 min, and then calcined at 550 °C for 10 h in the same atmosphere.

2.2. Characterization

The X-ray diffraction (XRD) measurement was carried out on a Bruker D8 Advance X-ray diffraction using Cu Kα radiation source (λ = 1.5406 Å) with a step size of 4° min^{-1} from 10° to 80°. The powder morphology was observed by scanning electron microscope (SEM) on JEOL JSM-6390.

The electrochemical performance of as-prepared $LiMnPO_4$ was investigated using coin cells assembled in an argon-filled glove box (SIMATIC OP7, MBRAUN). The cell was composed of a lithium anode and a cathode that was a mixture of prepared $LiMnPO_4$ (70%), Super P Carbon black (20%) and polytetrafluoroethylene (PTFE) (Dupont) (10%). The mixture was rolled into a thin sheet with uniform thickness, then it was cut into 10 × 10 mm section before being pressed to a aluminum mesh. Typical loading of the active material is about 10 mg cm^{-2}. The electrolyte was 1 M $LiPF_6$ dissolved in a mixed solvent of ethylene carbonate (EC) and dimethyl carbonate (DMC) (1:1 in weight), and Celgard 2300 was used as separator. The electrochemical charge–discharge measurements were carried out in the voltage range from 2.5 to 4.6 V vs. Li^+/Li on LAND CT 2001 cell test instrument (Wuhan Kingnuo Electronic Co, China). All the tests were performed at room temperature.

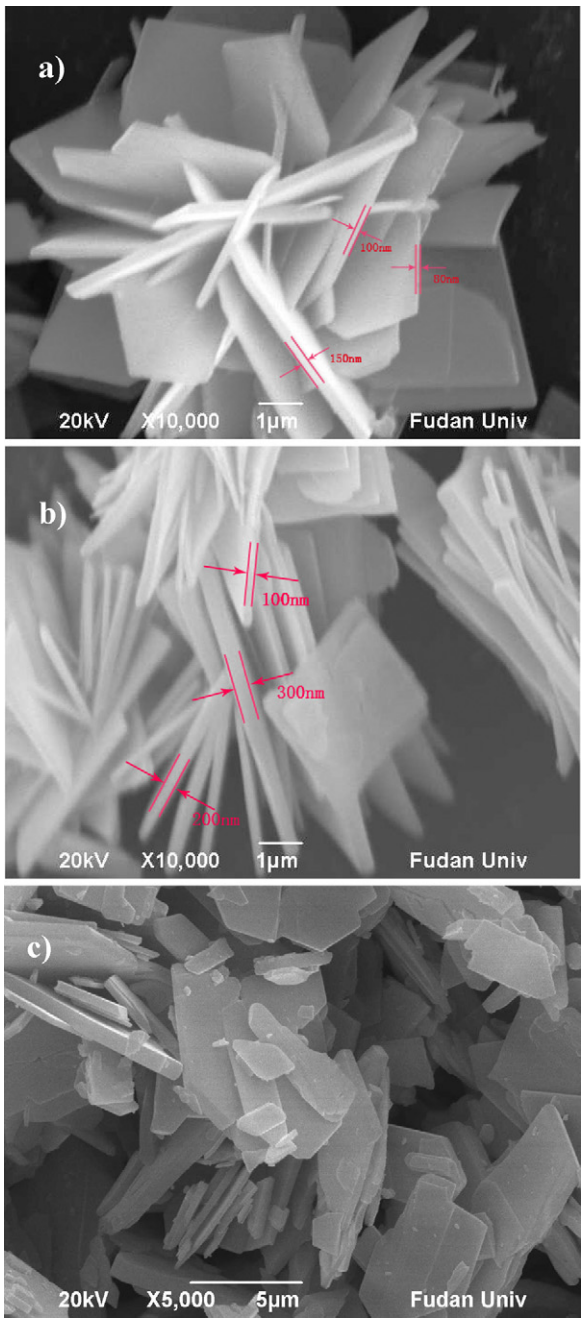

Fig. 2. The SEM photos of as-prepared $NH_4MnPO_4{\cdot}H_2O$, (b) with adding citric acid. (b) Without adding citric acid.

3. Results and discussion

3.1. Characterization of $NH_4MnPO_4{\cdot}H_2O$

The diffraction pattern of as-prepared $NH_4MnPO_4{\cdot}H_2O$ was displayed in Fig. 1(a). It could be concluded that all the diffraction peaks can be ascribed to Pmn2 structure without any impurities. And the sharp peak also indicated the high crystallization. The major lattice plane was emphasized in figure. It was worth mentioning that the peak intensity ratio of our sample showed some difference compared with the previous report [28]. It showed a strong orientation effect in (0 1 0) plane. To explore the forming

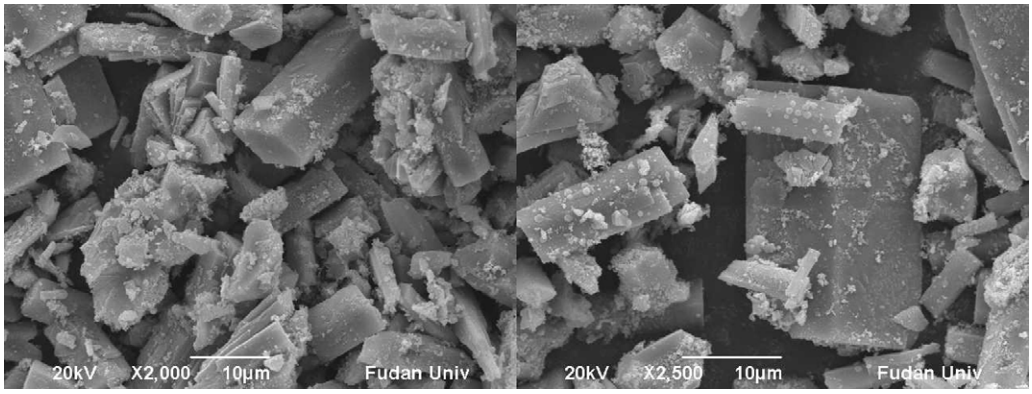

Fig. 3. The SEM photos of the manganese citrate complex.

mechanism, the white powder obtained after addition of citric acid was also characterized by XRD measurement, and it was marked as (b) in Fig. 1. It was visible that its diffraction peaks was more complicated than $NH_4MnPO_4{\cdot}H_2O$. Even though great efforts have been made to recognize the phase composition, we still cannot identify it exactly. However, the so-called manganese citrate chemistry was generally accepted to exist in the similar aqueous system [29,30]. It was believed that the composition for manganese citrate could be various, and the framework of the crystal structure would be different, respectively. Hence, we regarded this white powder as manganese citrate complexes.

The morphology of the $NH_4MnPO_4{\cdot}H_2O$ could be seen in the SEM photos as shown in Fig. 2(a). The sample apparently consists of plate-like crystallites whose thickness range from 100 nm to 300 nm. Islam used the advanced simulation techniques to analyze the crystal morphology of $LiFePO_4$ [31]. His group found that it (0 1 0) provides the lowest surface energy for plate-like morphology. This conclusion coincided with the orientation effect in our XRD data. According to the previous studies, the plates of $NH_4MnPO_4{\cdot}H_2O$ were prone to be irregular. However, it found that the plates all assembled to flower-like morphology in our as-prepared $NH_4MnPO_4{\cdot}H_2O$. For comparison, the SEM photo of $NH_4MnPO_4{\cdot}H_2O$ without adding citric acid was also shown in Fig. 2(b). It can be seen that the morphology was irregular plate-like rather than flower-like which consisted with the previous studies.

3.2. Reaction mechanism

To illustrate the formation mechanism, the SEM photos of manganese citrate complexes were also shown in Fig. 3. Compared to the flower-like morphology for $NH_4MnPO_4{\cdot}H_2O$, the huge rod-like particle ranging from 5 to 15 μm could be observed for this sample. Morphology change from rod-like to flower-like may be owed to the formation process of the $NH_4MnPO_4{\cdot}H_2O$. Here, we employed the solubility–reprecipitation equilibrium was depicted in the scheme as shown in Fig. 4 to interpret the mechanism in this process.

The huge-rod like particles with a size of 5–10 μm were produced after the citric acid was added into solution which contains Mn^{2+} in step I, through which the equilibrium of Eq. (1) was decomposed by subsequent adding of $NH_4H_2PO_4$ while the Ksp was temporarily unaccessible for precipitation of NH_4MnPO_4 in a solubility-precipitation balance in step II; Eq. (2) turned to be dominant by adding $NH_3{\cdot}H_2O$ and reprecipitation, in which particles were self-assembled to flower-like morphology, was finished in an adjustable pH value range from 10.2 to 10.7.

$$Mn^{2+} + \text{citrate} \leftrightarrow Mn(\text{citrate}) \quad (1)$$

$$NH_4^{+} + Mn^{2+} + PO_4^{3-} \leftrightarrow NH_4MnPO_4{\cdot}H_2O \quad (2)$$

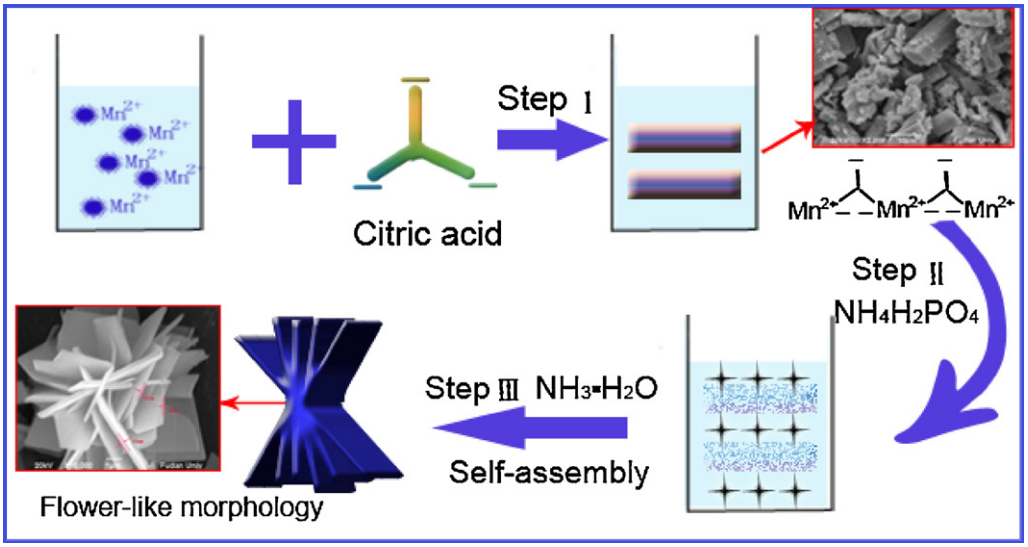

Fig. 4. The schematic diagram of the formation mechanism for $NH_4MnPO_4{\cdot}H_2O$.

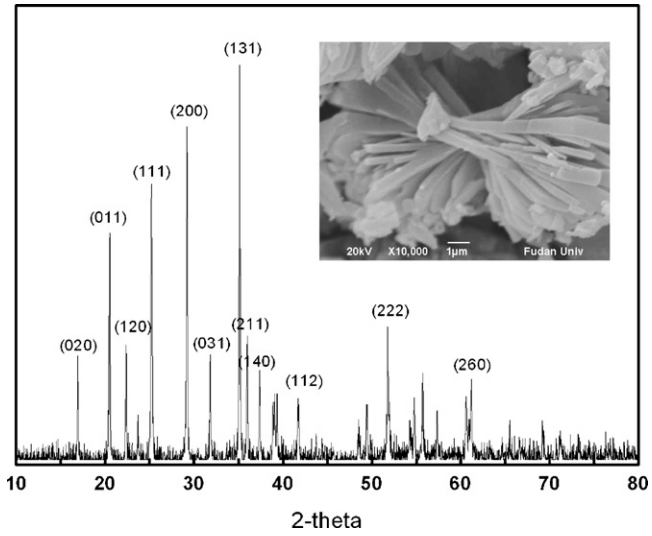

Fig. 5. The XRD patterns and SEM photo for obtained $LiMnPO_4$/C.

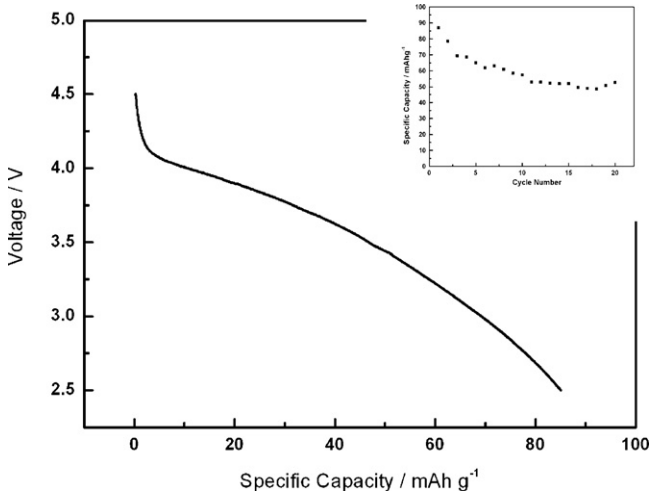

Fig. 6. The discharge curve and cycling performance for $LiMnPO_4$/C as the cathode material of LIB.

3.3. Characterization of $LiMnPO_4$

Fig. 5 showed the XRD diffraction for $LiMnPO_4$ obtained from the caclination of $NH_4MPO_4{\cdot}H_2O$ and LiAC. The major lattice planes were also remarked in figure. Because of the topological similarity between $NH_4MnPO_4{\cdot}H_2O$ and $LiMnPO_4$, the ion exchange of NH_4^+ to Li^+ should deliver little structure rearrangement [28]. All the diffraction peaks could be identified as the single phase of $LiMnPO_4$ without any impurities.

The SEM photos of $LiMnPO_4$/C were also displayed in Fig. 5. The flower-like morphology could still be obviously observed in the $LiMnPO_4$/C sample. According to previous literatures, it was generally considered that the morphology of NH_4MPO_4 (M = Fe, Co, Mn) could not be maintained during the solid-state reaction. Bramnik applied the molten $LiCl–LiNO_3$ to carry ionic exchange with $NH_4MnPO_4{\cdot}H_2O$ and his group found that the morphology of $NH_4MnPO_4{\cdot}H_2O$ would only be remained through this method [28]. However, in our experiment, the morphology could be successfully remained even through the solid-state reaction. It may ascribe to the relative low subsequent sintering temperature.

3.4. Electrochemical behavior of $LiMnPO_4$

The discharge plot of $LiMnPO_4$ as the cathode material of lithium ion battery was provided in Fig. 6. The charge and discharge tests were all conducted at 0.05 C, with a voltage range of 2.5–4.5 V and the discharge capacity was about 85 mAh g^{-1}. Instead of obvious flat voltage at approximately 4.1 V which indicated the two phase exchange between $LiMnPO_4$ and $MnPO_4$, it exhibited a slopping curve. The insert of Fig. 6 was the cycling performance of $LiMnPO_4$/C. The poor discharge capacity and cycling ability could be ascribed to the extremely low electronic conductivity combined with low Li^+ diffusion constant which were thought to be the key limitation for the family of $LiMPO_4$ (M = Fe, Mn). In particular, the much poorer electronic conductivity and the distortion of the Jahn–Teller active Mn^{3+} ion for $LiMnPO_4$ suggested that its energy could not be easily achieved. Moreover, the relative large particles also have disadvantage on the electrochemical performance. Hence, cation doping, carbon coating and particle size reduction were all believed to be effective ways to overcome these drawbacks. Besides, our future work would also focus on improving the electrochemical behavior of $LiMnPO_4$ by adjusting the morphology of its precursors.

4. Conclusion

In this work, we suggested a novel method to prepare flower-like $NH_4MnPO_4{\cdot}H_2O$ in the aqueous solution with manganese citrate complexes as the intermediate. The same morphology of $LiMnPO_4$/C composite could be obtained by traditional solid-state reaction with $NH_4MnPO_4{\cdot}H_2O$ as the precursor. The solubility–reprecipitation mechanism was successfully employed to illustrate the forming process of this particular morphology. This method may be useful for the synthesis of other functional materials. Due to the intrinsic low ionic and electronic conductivity, this flower-like $LiMnPO_4$/C composite delivered poor discharge capacity of 85 mAh g^{-1} at 0.05 C. This could be improved by cation doping, excellent carbon coating and our later studies would focus on this problem.

References

[1] A.K. Padhi, K.S. Nanjundaswamy, J.B. Goodenough, J. Electrochem. Soc. 144 (1997) 1188–1194.
[2] S.Y. Chung, J.T. Bloking, Y.M. Chiang, Nat. Mater. 1 (2002) 123–128.
[3] C.A.J. Fisher, V.M. Hart Prieto, M.S. Islam, Chem. Mater. 20 (2008) 5907–5915.
[4] C.L. Hu, H.H. Yi, H.S. Fang, B. Yang, Y.C. Yao, W.H. Ma, Y.N. Dai, Electrochem. Commun. 12 (2010) 1784–1787.
[5] Y.N. Xu, W.Y. Ching, Y.M. Chiang, J. Appl. Phys. 95 (2004) 6583–6585.
[6] S.K. Martha, B. Markovsky, J. Grinblat, Y. Gofer, O. Haik, E. Zinigrad, D. Aurbach, T. Drezen, D. Wang, G. Deghenghi, I. Exnar, J. Electrochem. Soc. 156 (7) (2009) A541–A552.
[7] C.A.J. Fisher, V.M.H. Prieto, M.S. Islam, Chem. Mater. 20 (2008) 5907–5915.
[8] H.H. Chang, C.C. Chang, H.C. Wu, Z.Z. Guo, M.H. Yang, Y.P. Chiang, H.S. Sheu, N.L. Wu, J. Power Sources 158 (2006) 550–556.
[9] J.C. Zheng, X.H. Li, Z.X. Wang, H.J. Guo, S.Y. Zhou, J. Power Sources 184 (2008) 574–577.
[10] M. Higuchi, K. Katayama, Y. Azuma, M. Yukawa, M. Suhara, J. Power Sources 119 (2003) 258–261.
[11] A.K. Padhi, K.S. Nanjundaswamy, C. Masquelier, J.B. Goodenough, J. Electrochem. Soc. 144 (1997) 1609–1613.
[12] A. Eftekhari, J. Electrochem. Soc. 151 (2004) A1816–A1819.
[13] A. Yamada, S.C. Chung, J. Electrochem. Soc. 148 (2001) A960–A967.
[14] A. Yamada, M. Hosoya, S.-C. Chung, Y. Kudo, K. Hinokuma, K.-Y. Liu, Y. Nishi, J. Power Sources 119–121 (2003) 232–238.
[15] F. Zhou, M. Cococcioni, K. Kang, G. Ceder, Electrochem. Commun. 6 (2004) 1144–1148.
[16] D.W. Choi, D.H. Wang, I.T. Bae, J. Xiao, Z.M. Nie, W. Wang, V. Viswanathan, Y.J. Lee, J.G. Zhang, G.L. Graff, Z.G. Yang, J. Liu, Nano Lett. 10 (2010) 2799–2805.
[17] A.M. Hashambhoya, J.F. Whitacrea, J. Electrochem. Soc. 158 (2011) A390–A395.
[18] C. Delmas, M. Maccario, L. Croguennec, F. Le Cras, F. Weill, Nat. Mater. 7 (2008) 665–671.
[19] S. Nishimura, G. Kobayashi, K. Ohoyama, R. Kanno, M. Yashima, A. Yamada, Nat. Mater. 7 (2008) 707–711.
[20] C. Delacourt, P. Poizot, J.-M. Tarascon, C. Masquelier, Nat. Mater. 4 (2005) 254–260.

[21] J.S. Kim, Y.U. Park, D.H. Seo, J. Kim, S.K. Kim, K. Kang, Electrochem. Soc. J. 158 (2011) A250–A254.
[22] K.F. Hsu, S.Y. Tsay, B.J. Hwang, J. Mater. Chem. 14 (2004) 2690–2695.
[23] M.S. Islam, D.J. Driscoll, C.-A.J. Fisher, P.R. Slatter, Chem. Mater. 17 (2005) 5085–5092.
[24] H.S. Fang, L.P. Li, Y. Yang, G.F. Yan, G.S. Li, Chem. Commun. (2008) 1118–1120.
[25] P. Barpanda, K. Djellab, N. Recham, M. Armand, J.M. Tarascon, J. Mater. Chem. 21 (2011) 10143–10152.
[26] W. Li, J. Gao, J. Ying, C. Wan, C. Jiang, J. Electrochem. Soc. 153 (2006) F194–F198.
[27] J. Lloris, C. PérezVicente, J. Tirado, Electrochem. Solid State Lett. 5 (2002) A234–A237.
[28] N. Bramnik, H. Ehrenberg, J. Alloys Compd. 464 (2008) 259–264.
[29] M. Matzapetakis, N. Karligiano, A. Bino, M. Dakanali, C.P. Raptopoulou, V. Tangoulis, A. Terzis, J. Giapintzakis, A. Salifoglou, Inorg. Chem. 39 (2000) 4044–4051.
[30] W.G. Wang, X.F. Zhang, F. Chen, C.B. Ma, C.N. Chen, Q.T. Liu, D.Z. Liao, L.C. Li, Polyhedron 24 (2005) 1656–1668.
[31] C. Fisher, M.S. Islam, J. Mater. Chem. 18 (2008) 1209–1215.